OXFORD

SOT | Society of Toxicology
www.toxsci.oxfordjournals.org

TOXICOLOGICAL SCIENCES, 152(1), 2016, 128–144

doi: 10.1093/toxsci/kfw068
Advance Access Publication Date: April 28, 2016
Research Article

Effects of Polyamidoamine Dendrimers on a 3-D Neurosphere System Using Human Neural Progenitor Cells

Yang Zeng,*,† Yoshika Kurokawa,* Qin Zeng,* Tin-Tin Win-Shwe,†,‡ Hiroko Nansai,* Zhenya Zhang,† and Hideko Sone*,[1]

*Center for Environmental Risk Research, National Institute for Environmental Studies, 16-2 Onogawa, Tsukuba, Ibaraki, 305-8606, Japan; †Department of Life and Environmental Science, Major of Bioindustrial Sciences, the University of Tsukuba, 1-1-1 Tennodai, Tsukuba, Ibaraki, 305-0006, Japan; and ‡Center for Environmental Health Sciences National Institute for Environmental Studies, 16-2 Onogawa, Tsukuba, Ibaraki, 305-8606, Japan

[1]To whom correspondence should be addressed at Research Center for Environmental Risk, National Institute for Environmental Studies, 16-2 Onogawa, Tsukuba, Ibaraki 305-8506, Japan. Fax: +81-29-850-2546. E-mail: hsone@nies.go.jp.

ABSTRACT

The practical application of engineered nanomaterials or nanoparticles like polyamidoamine (PAMAM) dendrimers has been promoted in medical devices or industrial uses. The safety of PAMAM dendrimers needs to be assessed when used as a drug carrier to treat brain disease. However, the effects of PAMAM on the human nervous system remain unknown. In this study, human neural progenitor cells cultured as a 3D neurosphere model were used to study the effects of PAMAM dendrimers on the nervous system. Neurospheres were exposed to different G4-PAMAM dendrimers for 72 h at concentrations of 0.3, 1, 3, and 10 μg/ml. The biodistribution was investigated using fluorescence-labeled PAMAM dendrimers, and gene expression was evaluated using microarray analysis followed by pathway and network analysis. Results showed that PAMAM dendrimer nanoparticles can penetrate into neurospheres via superficial cells on them. PAMAM-NH_2 but not PAMAM-SC can inhibit neurosphere growth. A reduced number of MAP2-positive cells in flare regions were inhibited after 10 days of differentiation, indicating an inhibitory effect of PAMAM-NH_2 on cell proliferation and neuronal migration. A microarray assay showed 32 dendrimer toxicity-related genes, with network analysis showing 3 independent networks of the selected gene targets. Inducible immediate early gene early growth response gene 1 (Egr1), insulin-like growth factor-binding protein 3 (IGFBP3), tissue factor pathway inhibitor (TFPI2), and adrenomedullin (ADM) were the key genes in each network, and the expression of these genes was significantly down regulated. These findings suggest that exposure of neurospheres to PAMAM-NH_2 dendrimers affects cell proliferation and migration through pathways regulated by Egr1, IGFBP3, TFPI2, and ADM.

Key words: PAMAM dendrimers; human neural progenitor cells; neural development; nano toxicology.

Dendrimers are at the forefront of research in nanoscience because of several interesting macromolecular system properties, such as their precise architecture, high uniformity and purity, high loading capacity, and high shear resistance (Newkome *et al.*, 1998). They have shown a great deal of versatility with applications in various areas such as drug delivery, medical therapy, electrochemistry, metal recovery, and sensors (Bharatwaj *et al.*, 2014; Khodadust *et al.*, 2014).

Polyamidoamine (PAMAM) dendrimers are a common type of dendrimers that have a radial structure consisting of a 2-carbon ethylenediamine core and functional groups on their surfaces. These functionalized surface groups can be easily

changed, enabling their wide use in biological applications such as drug (Cui *et al.*, 2009) or gene delivery (Huang *et al.*, 2007; Ke *et al.*, 2009). It has been reported that large cationic dendrimers, but not anionic, neutral, or small cationic dendrimers, induce aggregation of human platelets in plasma *in vitro* (Dobrovolskaia *et al.*, 2012). The toxicity of PAMAM dendrimers has increased with later generations; EC50 for G4 PAMAM dendrimers-NH_2 was 5–20 μM (Mukherjee *et al.*, 2010a), and toxicity was also correlated linearly with the zeta potential of dendrimers in mammalian cells (Mukherjee *et al.*, 2010b). To use PAMAM dendrimers as a drug carrier in treating brain disease, PAMAMs need to reach the parenchyma of the brain. An *in vivo* study has shown that PAMAM is essentially unable to affect the mature brain after a single intranasal instillation because it is blocked by the blood-brain barrier (Win-Shwe *et al.*, 2014). However, the distribution of dendrimer and hal operidol in the brain was significantly increased compared with a control of haloperidol when administered via intraperitoneal injection (Katare *et al.*, 2015). Moreover, PAMAM dendrimers can cross the cell membrane and reach an intracellular localization after a 2 μl intracerebroventricular injection of dendrimers G4 in a mouse at a concentration of 10 μM (Albertazzi *et al.*, 2013). Therefore, the safety of PAMAM dendrimers needs to be assessed when used as a drug delivery agent.

To assess PAMAM dendrimer toxicity on the human brain after intracerebroventricular injection, an *in vitro* study is first needed to assess the neurotoxicity of PAMAM dendrimers on neuronal cells. Previous studies have shown that the embryonic stem cell models can be used to assess developmental neurotoxicity. The effect of valproic acid on neurodevelopment has also been studied by regulating gene expression and analyzing gene pathways (Schulpen *et al.*, 2015a). In addition, the response of 2 anticonvulsant drugs on gene expression in human embryonic stem cells has been analyzed (Schulpen *et al.*, 2015b). However, most agents cannot be identified with certainty. This is because 2D models do not reflect the basic processes occurring during fetal brain development. A 3D neurosphere model should therefore be used. The neurosphere model has the following advantages: convenient; efficient; similar to the *in vivo* situation; improves cell interactions; and better reflects the basic processes of fetal brain development, such as proliferation, differentiation, and apoptosis. Differentiating Ntera2/clone D1 cell neurospheres were exposed to human teratogens, such as acrylamide, to test their developmental neurotoxicity, and it was found that the neurosphere model of neurogenesis may provide the basis for a model of developmental neurotoxicity *in vitro* (Hill *et al.*, 2008). Neurosphere assays have been also used to compare human and rat developmental neurotoxicity, and it was also found that a neurosphere model is a good tool to study developmental neurotoxicity in humans and rats (Baumann *et al.*, 2014; Zeng *et al.*, 2015). In our study, a 3D neurosphere model based on human neural progenitor cells (hNPCs) was used to assess the neurotoxicity of PAMAM dendrimers. We investigated the migration of cells from the neurosphere core. We also investigated the biodistribution of PAMAM dendrimers in the neurosphere and the effect of PAMAM dendrimers on the neurosphere. We used fluorescence-labeled PAMAM dendrimers to investigate their biodistribution in a 3D cell culture model by exposing these dendrimers to 3D neurospheres and found a time-dependent biodistribution of the dendrimers. To the best of our knowledge, this is the first study to evaluate the developmental neurotoxicity of PAMAM dendrimer nanoparticles in a 3D cell culture model.

MATERIALS AND METHODS

Dendrimers

PAMAM (ethylenediamine core, generation 4.0; Cat. No. 664049-1KT) 10 wt.% methanol solution and PAMAM G4-SC, which was modified with sodium carboxylate surface groups, (10 wt.% in methanol, 412430-2.5G) were purchased from Sigma-Aldrich (St Louis, Missouri). PAMAM was conjugated with an Alexa 546 fluorophore to prepare infrared-labeled PAMAM dendrimers. Conjugation was synthesized via an amide bond between the primary amine of the dendrimer and the N-hydroxysuccinimide-activated carboxyl of the fluorophore. PAMAM G4 stock solution (20 mg) was combined with 0.1 M Alexa Fluor 488 or Alexa Fluor 546 carboxylic acid, succinimidyl ester (Invitrogen., Eugene, Oregon) at pH 8.3. The reaction was allowed to proceed under stirring for 3 h at room temperature (RT). The product was purified using a Slide-A-Lyzer Dialysis Cassette (Thermo Scientific., USA) with a 3500 Dalton cut off to remove free fluorophore.

Particle Characteristics

The dendrimer test solutions were prepared in neural expansion media (NEM) at 37°C under a low-speed vortex. The size and zeta potential of the dendrimers at different concentrations (1, 3, and 10 mg/ml) were measured using ELSZ-2000 (Otsuka Electronics Co., Ltd. Japan). The conjugation of the Alexa 488 and PAMAM-Alexa 488 was characterized using TOF–TOF MALDI–TOF–MS (Axima Performance, Shimadzu, Japan).

Reagents for Cell-Based Assays

L-glutamine, poly-L-ornithine, and laminin from engelbreth-holm-swarm (laminin -111) were provided by Sigma-Aldrich (Japan). Human recombinant laminin (laminin-511) was obtained from BioLaminaAB (Stockholm, Sweden). NEM was obtained from ENStem-A. Neurobasal medium and Glutamax were purchased from Life Technologies (Gibco; USA). hNPCs derived from H9 human embryonic stem cells were obtained from Chemicon-Millipore (ENStem Human Neural Progenitor Expansion Kit; Norcross, Georgia, USA). All experiments using hNPCs were approved by the ethics committees of the National Institute for Environmental Studies and were conducted in accordance with the guidelines of the Japanese Ministry of Education, Culture, Sports, Science, and Technology.

Neurosphere Formation and Incorporation of Alexa-Labeled PAMAM Dendrimers

hNPCs were cultured in NEM (ENStem-A) supplemented with 0.05% b-FGF and 1% L-glutamine (Sigma-Aldrich, St Louis, Missouri) on polyornithine-coated (Sigma-Aldrich, St Louis Missouri) and laminin-111-coated (Sigma-Aldrich, St Louis, Missouri) dishes. On day 0 (d0), the cells were transferred to 96-well round bottom plates (Nunc, Falcon) at a density of 6000 cells per well to allow neurosphere formation; this 3D culture system has been established in our previous study Zeng *et al.* (2015).

Alexa 546-labeled PAMAM dendrimers at a concentration of 10 μg/ml were incubated with the neurospheres in 96-well round bottom plates on d2. The spheres were transferred to a laminin-511-coated glass bottom dish for observation on d3–d5. Microphotographs showing the incorporation of Alexa 546-labeled PAMAM dendrimers were obtained using an Olympus

LV1200 high-performance laser scanning microscope (Olympus Optical, Japan). Images for illustration were obtained using 10× and 20× objectives. 3D images were created using the FV10-ASW software (Olympus Optical, Japan) with 7 images per stack. The thickness of each stack was 3 μm.

Immunofluorescence and Morphological Analysis

To investigate neurosphere proliferation, migration, and differentiation, on d2, 3 doses of PAMAM dendrimers (1, 3, and 10 μg/ml) were exposed for 72 h in both NEM and neural differentiation media (NDM). The doses were determined based on our previous study Zeng *et al.* (2016a,b)

On d5), neurospheres were transferred to NEM (ENStem-A) supplemented with 0.05% b-FGF and 1% L-glutamine (Sigma-Aldrich, St Louis Missouri) on polyornithine-coated (Sigma-Aldrich, St Louis Missouri) and laminin-111-coated (Sigma-Aldrich, St Louis Missouri) 48-well plates. On d7, a Plus EdU Alexa Fluor imaging kit (Thermo Fisher Scientific, Tokyo, Japan) was used to label newly synthesized DNA in hNPCs for 24 h. On d8, cells were then treated with 2 g/ml of Hoechst 33342 solution for 15 min at RT to label all cell nuclei. Immunofluorescence images were acquired using an FV1200 microscope (Olympus, Tokyo, Japan). Sphere area was assessed using Image J. A sphere was identified manually, and the area was calculated by the software.

To investigate neurosphere differentiation, the neurospheres were gently transferred to a 48-well plate precoated with laminin-511 and containing NDM supplemented with 1× B27, 1× N2, and 10 ng/ml BDNF (Invitrogen, Carlsbad, California). NDM was changed every 3 days. Immunostaining was performed on d10. Neurospheres were fixed using 4% paraformaldehyde for 15 min and then treated with 0.1% Triton X-100 for 30 min. After incubating with 1% BSA–PBS for 30 min at RT, cells were treated with primary antibodies (mouse anti-microtubule-associated protein 2 [MAP2; 1:200 dilution; Sigma-Aldrich]) overnight at 4°C. After washing with PBS, the cells were incubated with secondary antibodies (Alexa Fluor 488 donkey anti-mouse lgG; 1:1000 dilution) for 1 h at RT. Following this, the cells were treated with 2 μg/ml Hoechst 33342 solution for 15 min at RT. Neurite length per cell and nuclei number were analyzed and calculated using an InCell analyzer 1000 (GE Healthcare, Tokyo, Japan). Images were obtained using a 10× objective, and nine images were acquired for each well. Sphere area and neurite migrations were investigated using Image J.

Microarray Analyses and Bioinformatics

On d2, neurospheres for microarray were treated with PAMAM dendrimer-NH2 (0.3 μg/ml) for 72 h. Four neurospheres from different experimental groups were pooled together separately. RNAs were isolated from each group on d5. To detect changes in gene expression in neurospheres after PAMAM dendrimer exposure, microarray analyses were performed on 2 RNA samples using a microarray (Sureprint G3 Human GE 8 × 60K Ver.2.0 1color 4; Agilent Technologies Inc., Santa Clara, Californnia). The arrays were hybridized and scanned in accordance with the manufacturer's directions at the facility of Hokkaido System Science Co., Ltd. (Sapporo, Japan). The raw data were normalized and filtered by comparing expression levels to the cut-off low values and then filtered by flag tag to remove entities that were not detected using GeneSpring GX12.10 software (Agilent Technologies). The microarray data were submitted to Gene Expression Omnibus and registered as GSE65875 (http://www.ncbi.nlm.nih.gov/geo/query/acc.cgi?acc=gse65875, last accessed Apr 29, 2016). Genes with fold changes in $\log_2$ expression values of >1.5 or ≤ 1.5 from each group were selected and combined to generate a common entity list. Genes from the commonly responsive list were analyzed using Single Experiment Analysis (SEA) of GeneSpring to find matching genes in WikiPathways. Matched gene entities from the top 5 pathways were selected; these 12 genes were then analyzed using the natural language processing (NLP) network analyses of GeneSpring to identify extended interactions.

Quantitative Gene Expression Assay

To confirm gene expression, on d2, neurospheres for RT-PCR were treated with PAMAM dendrimer-NH_2 (0.3, 1, and 3 μg/ml) for 72 h. RNAs were isolated from each group on d5. RNAs were extracted and purified using the RNeasy Micro kit (Qiagen, Hilden, Germany) according to the manufacturer's protocol. The RNA quality and quantity were then examined using a 2100 Bioanalyzer (Agilent Technologies, Santa Clara, California). A High-Capacity RNA-to-cDNA kit (Applied Biosystems, Foster, California) was used for RNA reverse transcription. Power SYBR Green PCR Master Mix (Applied Biosystems, Foster, California) and a MicroAmp Optical 96-Well Reaction Plate were used for real-time PCR with the 7000 Sequence Detection System (ABI PRISM, Foster City, USA). The following primer sets were used: TFPI2, 5′-TTCAGACTGAGGCTTCTATGGG-3′ (forward) and 5′-GTAAAACGACGGCCAGTTGAAGATACAGCTACCGTCTACTGC-3′ (reverse); Spry1, 5′-GTAAAACGACGGCCAGTGCGGTTTAGGCAATTTGTGATT-3′ (forward) and 5′-CCCTGGCATTACTTGGGAGT-3′ (reverse); EGR2, 5′- AGCTTTGCTCCCGTCTCTG-3′ (forward) and 5′-AGCTGGCACCAGGGTACT-3′ (reverse); insulin-like growth factor-binding protein 3 (IGFBP3), 5′-AGAGCACAGATACCCAGAACT-3′ (forward) and 5′-TGAGGAACTTCAGGTGATTCAGT-3′ (reverse); ADM, 5′-ACTTCGGAGTTTTGCCATTG-3′ (forward) and 5′-CTCTTCCCACGACTCAGAGC-3′ (reverse); KCNJ2, 5′-TGTTTTCCAAAGCAGAAGCA-3′ (forward) and 5′-CCCATCTTGACCAGTACCGT-3′ (reverse).

Statistical Analysis

Quantitative data were expressed as the percentage of control ± SD from at least 3 independent experiments. Analyses were performed using SPSS statistics v.19 (IBM, Tokyo, Japan). Statistical significance was determined by 1-way ANOVA, followed by the Dunnett's tests for pairwise comparisons. Differences were considered statistically significant when $P < .05$.

RESULTS

Particle Characteristics

We first characterized the properties of the nanomaterials. The diagram for the size distributions of high concentration PAMAM dendrimers and NEM is shown in Figure 1. The average particle sizes of NEM and the PAMAM dendrimers in the culture medium are shown in Table 1. It shows 2 or 3 peaks in the distribution of particles for all the PAMAM dendrimers, suggesting that secondary and tertiary aggregates after PAMAM dendrimers are mixed with NEM.

The zeta potential of the PAMAM dendrimers was measured in culture medium (Table 2). The zeta potential of culture medium was −33.93 mV. The zeta potential increased after all the PAMAM dendrimers aggregated with culture medium. High-concentration dendrimers showed a high zeta potential.

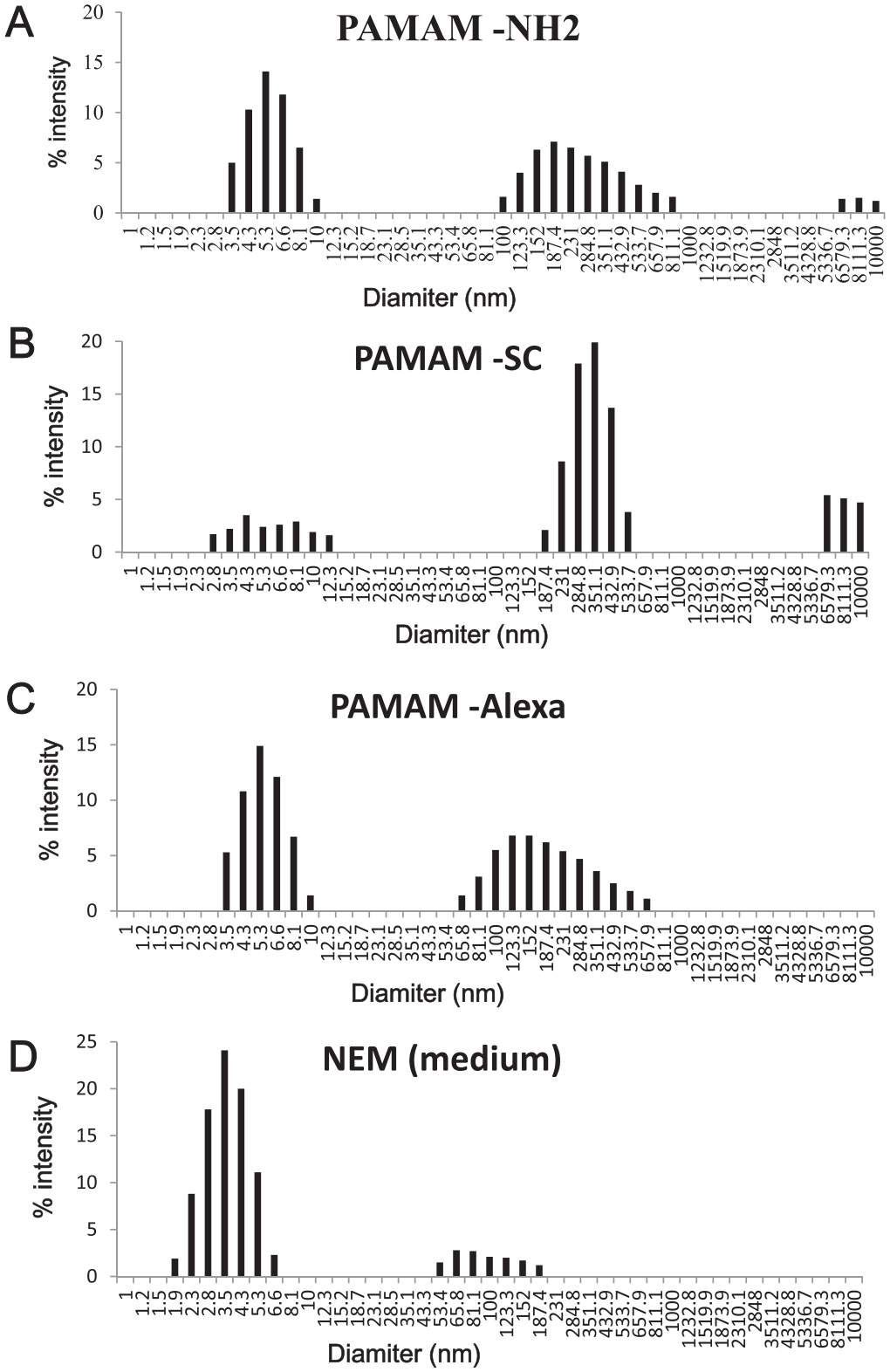

FIG. 1. Size distribution diagrams of PAMAM dendrimer-HN2 **(A)**, PAMAM dendrimer-SC **(B)**, and PAMAM dendrimer-Alexa 488 **(C)** at a concentration of 10 μg/ml in NEM and NEM **(D)**.

The conjugation of the Alexa 488 and PAMAM-Alexa 488 was characterized using TOF–TOF MALDI–TOF–MS. MS spectra of Alexa 488-PAMAM is shown in Supplementary Figure 1, and Alexa Fluor 488 is shown for comparison. Multiple signals not detected on Alexa Fluor 488 are detected on Alexa Fluor 488-PAMAM, although a intensity signal at M/Z 535.58 was detected (1a, 1b). Signals of Alexa Fluor 488 (M/Z 643.9) were not detected on Alexa 488-PAMAM(1c). Because multiple signals were

TABLE 1. Diameters of PAMAM Dendrimers and Culture Media

PAMAM Dendrimers	Concentration (μg/ml)	Mean Diameter (nm)
PAMAM-NH_2	1	26.1
	3	38.2
	10	104.8
PAMAM-SC	1	45.3
	3	173.4
	10	267.7
PAMAM-Alexa	1	18.4
	3	30.4
	10	45.4
NEM		6.9

TABLE 2. Zeta Potential Measurements of PAMAM Dendrimers

PAMAM Dendrimers	Concentration (μg/ml)	Zeta Potential (mV)
PAMAM-NH_2	1	−17.46 ± 0.42
	3	−13.88 ± 1.45
	10	−9.54 ± 1.61
PAMAM-SC	1	−21.36 ± 0.43
	3	−1.30 ± 0.44
	10	−17.54 ± 0.23
PAMAM-Alexa	1	−31.20 ± 2.45
	3	−18.38 ± 1.27
	10	−14.62 ± 2.25
NEM		−33.93 ± 2.83

detected in the Alexa 488-PAMAM, analysis using linear mode was used to assess whether a signal is detected in the high-molecular weight region with high sensitivity (low resolution). The MS spectrum of Alexa 488-PAMAM are shown in Supplementary Figure 2, and the MS spectrum of DHB (20 mg/ml DHB in 50% methanol solution) were used as a control. Multiple signals from Alexa 488-PAMAM were detected over a wide range of up to M/Z 9000.

Neurosphere Assay

We developed a 3D cell culture model to evaluate the effects of PAMAM dendrimers (Figure 2A). The process schedule was based on our previous study Zeng *et al.* (2015). For neurosphere formation, neurospheres were cultured in uncoated, round bottom plates from d0 to d2 (Figure 2C). Human progenitor cells formed spheres during 3D cell culture, and exposure to PAMAM dendrimers was conducted for 3 days after sphere formation from d2 to d5. After transfer to NDM media, spheres grew and neurite cells migrated. After plating for adhesion, polarized individual cells migrated outward from the spherical center after 24 h. On d5, the cell body size and projection length increased (Figure 2D); on d10, cellular projections increased not only in size but also in density (Figure 2E). Individual cells displayed multiple neurite outgrowths and dendritic spines, which are typical characteristics of both the immature and mature neuronal phenotype (Figure 2F).

Incorporation of PAMAM Dendrimers in Neurospheres

To examine the incorporation of PAMAM dendrimers into neurospheres, Alexa-PAMAM conjugates were incubated with neurospheres for 3 days. We used Alexa 488-conjugates in the sphere assays, but not Alexa 546 for intra-sphere distribution, because the fluorescence activity of Alexa 488 is weaker than that of Alexa 546. We could not obtain a clear picture from Alexa 488 distributions because of the sphere thickness. To confirm that free fluorescent agent was not taken up by neurospheres, a group of neurospheres were treated with PAMAM dendrimers for 3 days and then treated for 72 h with the fluorescent agent only. No fluorescent signal was observed in the neurospheres. For the Alexa-PAMAM conjugate-treated group, Alexa-PAMAM conjugate was incubated with neurospheres on d2. Cross-section images of neurospheres are shown in Figures 3A–C. The 3D images were generated using cross-section images, and 3D images were reversed to show the center of the neurospheres (Figs. 3D–F). The Alexa 546 fluorescence signal was only observed on the surface of neurospheres on d3 (Figs. 3A and D), and an increasing number of Alexa-PAMAM conjugates was observed within the neurospheres on d4 (Figs. 3B and E) and d5 (Figs. 3C and F). The results showed a time-dependent bio-distribution of PAMAM dendrimers and serve as evidence that Alexa-PAMAM was located in the center of neurospheres after 3 days of exposure.

Effect of PAMAM Dendrimers on the Proliferation and Migration of Neurospheres

To study the effect of PAMAM dendrimers on proliferation, newly synthesized DNA of hNPCs was fluorescently labeled with EdU and nuclei were labeled with Hoechst 33342. Representative images (4×) of PAMAM dendrimers are shown in Figures 4A–L. To quantify the effects of the dendrimers, neurosphere areas were measured using Image J. The mean area of the neurospheres decreased compared with that observed in the controls (Figure 4M). To confirm the inhibitory effect on cell proliferation, higher magnification images (10×) were acquired (Figure 5). Proliferation of cells in flare areas, which shifted from the neurosphere core, was investigated. These cells were considered as newly generated cells after PAMAM exposure. The EdU positive cell number decreased in the flare area, suggesting that PAMAM dendrimer inhibits both migration and cell proliferation.

Effect of PAMAM Dendrimers on Neuronal Differentiation of Neurospheres

To study the developmental neurotoxicity of PAMAM dendrimers, the neurites from the neurospheres were immunohistochemically stained with anti-MAP2 protein antibody on d10. The typical effects of PAMAM dendrimers are shown in Figures 6A–L. To quantify the effects of the dendrimers, the central core sizes of the neurosphere without flare areas and the flare areas that indicated cell migration and proliferation were measured using ImageJ software. The PAMAM dendrimer-NH_2 significantly inhibited both cell migration and proliferation in a dose-dependent manner. The mean area of the extended neuron decreased compared with that observed in the controls (Figure 6M). Alexa-PAMAM at a concentration of 3 and 10 μg/ml-inhibited cell migration (Figs. 6K and L); the extent of inhibition was similar to that observed using PAMAM-NH_2 dendrimers (Figs. 6C and D); however, Alexa-PAMAM conjugates did not affect migration or differentiation, whereas PAMAM-NH_2 dendrimers had an effect at a concentration of 1 μg/ml (Figs. 6B and J), suggesting that the surface group (NH_2) is important in explaining PAMAM toxicity. PAMAM-SC did not exert similar effects on MAP2-positive neurospheres at any test concentration (Figs. 6E–H).

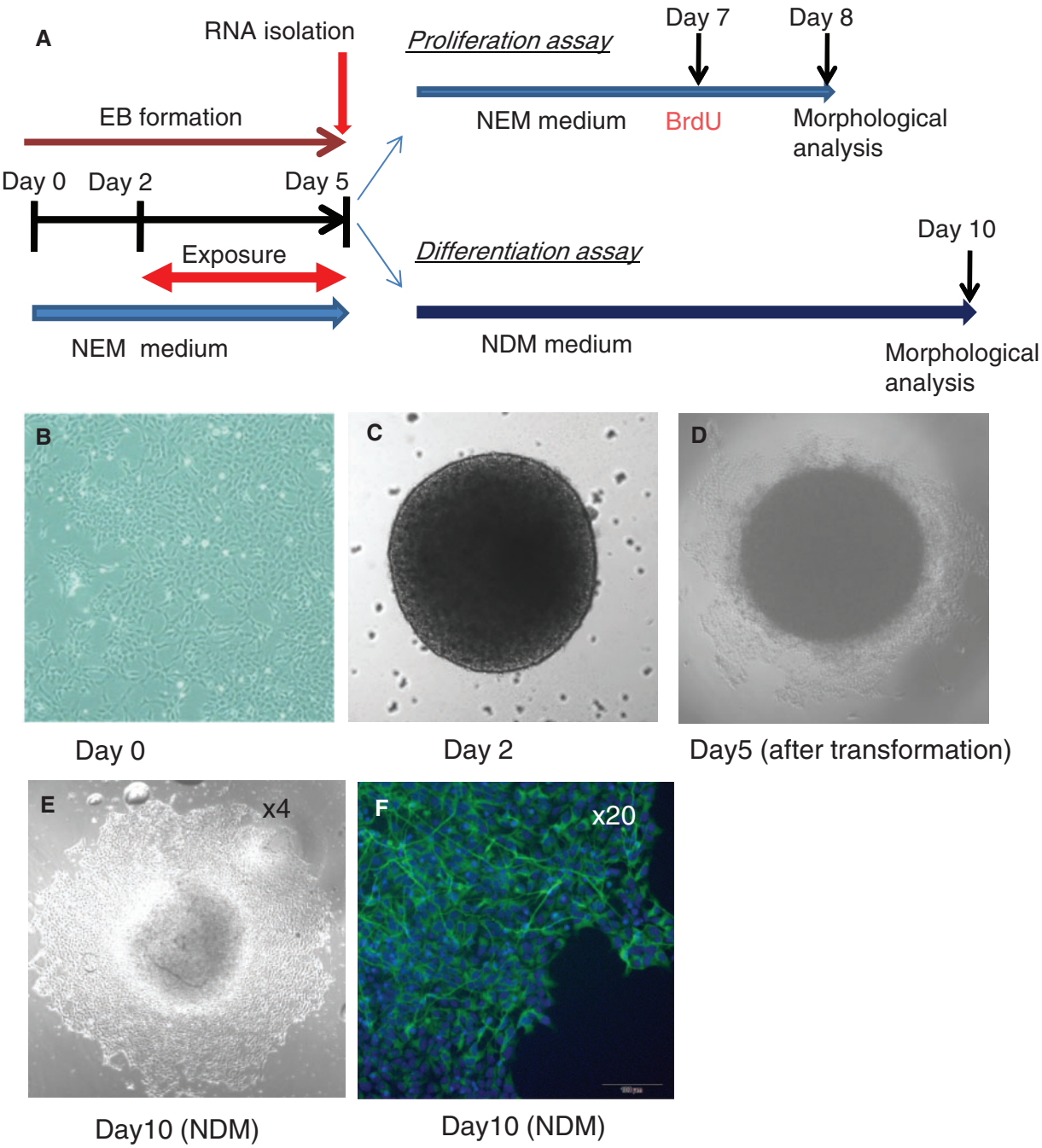

FIG. 2. Experimental time schedules of PAMAM exposure, proliferation, and differentiation **(A)**. Cells were seeded on d0 to form neurospheres and were exposed to different PAMAM dendrimers from d2 to d5. Gene expression analysis was conducted using total RNA from neurospheres on d5, followed by a proliferation assay from d5 to d8. The differentiation assay was performed from d5 to d10. Images of cell morphology for proliferation and differentiation of hNPCs in the neurosphere assay **(B–F)**.

The effects of PAMAM dendrimers on neurite length per cell and nuclei number that migrated from neural spheres were investigated (Figure 7A) and quantitatively determined. However, the dendrimers did not inhibit neurite length per cell at any concentration tested in this study. In contrast, neurite length per cell significantly increased at concentration of 10 μg/ml (Figure 7B), which may have been because the small cell density led to long neurites, as a decreased number of live cells were observed after exposure to PAMAM-NH_2 (Figure 7C).

Gene Expression Profiling in PAMAM dendrimer-Exposed Spheres by Microarray Analyses and RT-PCR

The expression of 50 739 genes was detected by microarray analysis after PAMAM dendrimer exposure. Genes that were either not detected or had a low expression value were filtered, leaving behind 25 622 genes. With fold changes in $\log_2$ expression values of >1.5 or ≤ 1.5, 289 and 171 of the entities were filtered from 2 independent experiments, respectively. Thirty-two of these genes were responsive in both experiments (Figure 8A), and their fold changes values are shown in Figure 8B. These 32

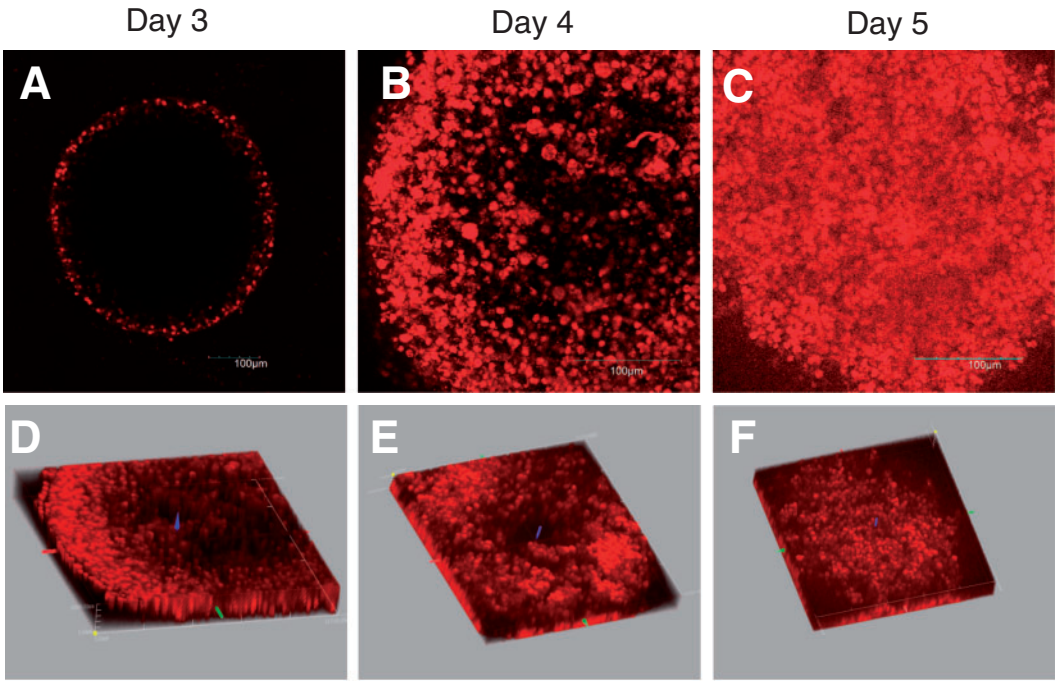

FIG. 3. Images of the distribution of PAMAM-NH_2 dendrimers using a confocal laser microscope. 2D images of a cross-section of a sphere **(A–C)** and 3D images **(D–F)** were acquired on d3 (A, D), d4 (B, E), and d5 (C, F) after starting sphere formation. 3D images (D–F) were located from the top of the sphere to the center with a thickness of 30 µm.

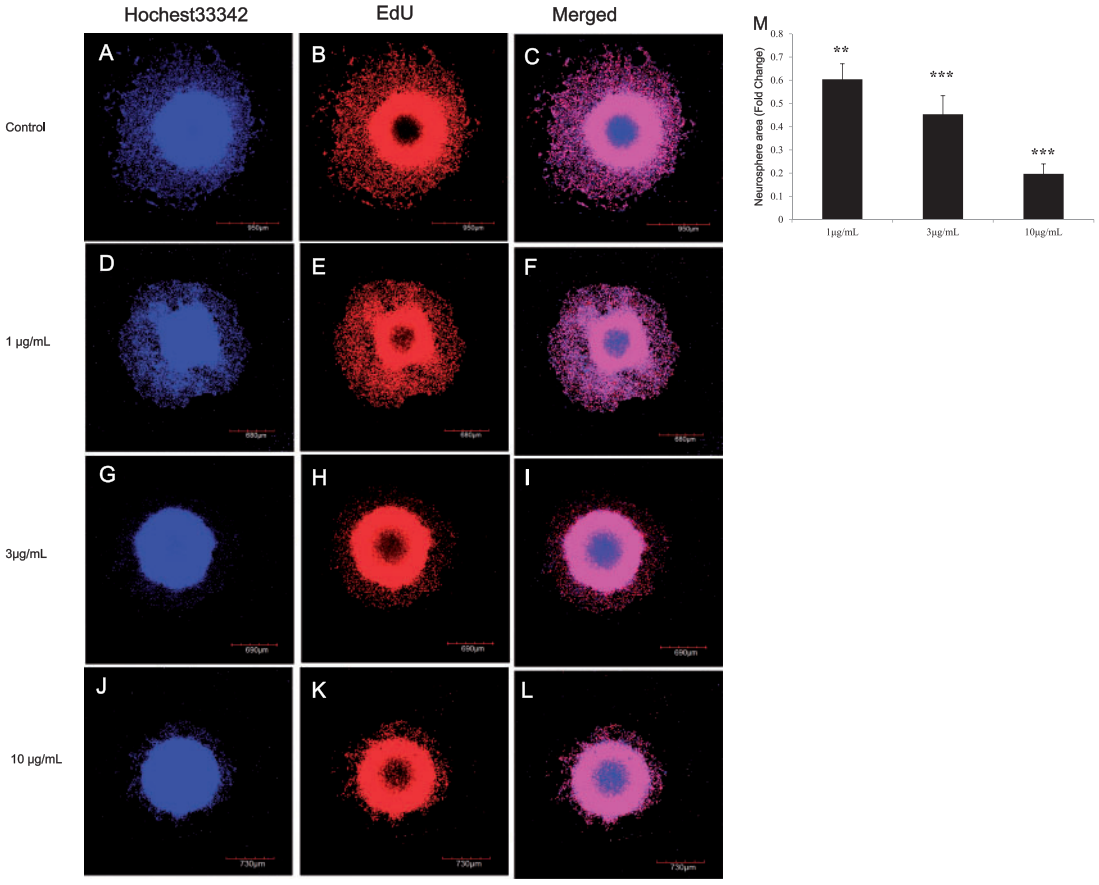

FIG. 4. Effects of PAMAM dendrimers on the migration and proliferation of neurospheres. Representative images were acquired on d8 following PAMAM-NH_2 treatment at concentrations of 1, 3, or 10 µg/ml for 72 h. Nuclei were stained with Hoechst 33342 **(A, D, G, J)**, and newly generated cells from d7 to d8 were labeled by EdU (Alexa 555 fluorescence) **(B, E, H, K)**. Quantified data on the effects on cell proliferation and migration of PAMAM-NH_2 were acquired using Image J by measuring sphere area **(M)**. Data are expressed as the percentage of control ± SD for 4 independent experiments. $^{**}P < .01$, and $^{***}P < .001$ were considered to be statistically significant differences between the treatment group and the vehicle control.

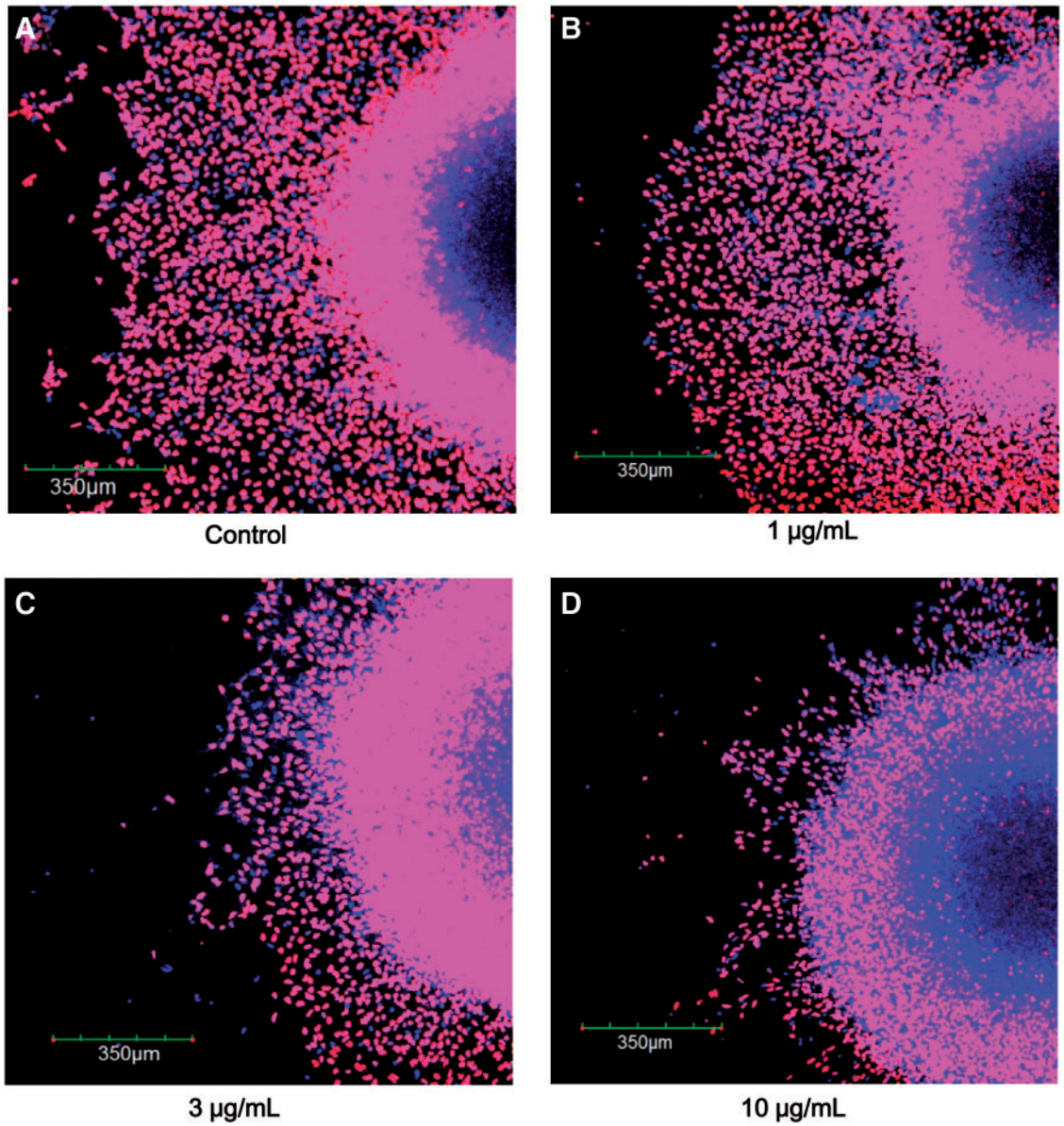

FIG. 5. High magnification images (10×) of merged with Hoechst 33342 and BrdU (Alexa 555 fluorescence) were acquired for control (**A**) and PAMAM-NH_2 treatment at concentrations of 1 (**B**), 3 (**C**), or 10 μg/mL (**D**) for 72 h.

genes were then analyzed by SEA to find matching genes in WikiPathways. Pathway analysis showed that direct interactions, network targets and regulators pathway, and Hs_Adipogenesis were the most matched pathways (Table 3). The matched gene expressions are shown in Table 4. Most of the matched genes, except CYP26A1, were down regulated. We then analyzed how the genes interact with each other using a NLP method. The result revealed 3 independent networks. Early growth response gene 1 (EGR1) (Figure 9A), IGFBP3 (Figure 9B), tissue factor pathway inhibitor (TFPI2), and ADM (Figure 9C) were the key nodes in each network. Therefore, the expression of these key genes (TFPI, SPRY2, IGFBP3, KCNJ2, ADM, and EGR1) was then confirmed using RT-PCR (Figure 10). All selected genes, except EGR1, were down regulated from a concentration of 1 μg/ml.

DISCUSSION

To assess how PAMAM dendrimer may affect the migration and differentiation of cells during development of the human nervous system, we used an hNPCsi-based neurosphere system. To the best of our knowledge, this is the first study to profile the gene response of neurospheres following PAMAM dendrimer exposure using microarray analysis. This showed the mechanism of how cationic PAMAM dendrimers-NH_2 may affect neurosphere development.

A few studies have reported the effects on cells following exposure to PAMAM dendrimers. For example, an *in vitro* study suggested that PAMAM induced the aggregation of human platelets in plasma (Dobrovolskaia *et al.*, 2012). Cationic but not anionic PAMAM dendrimers have been shown to induce

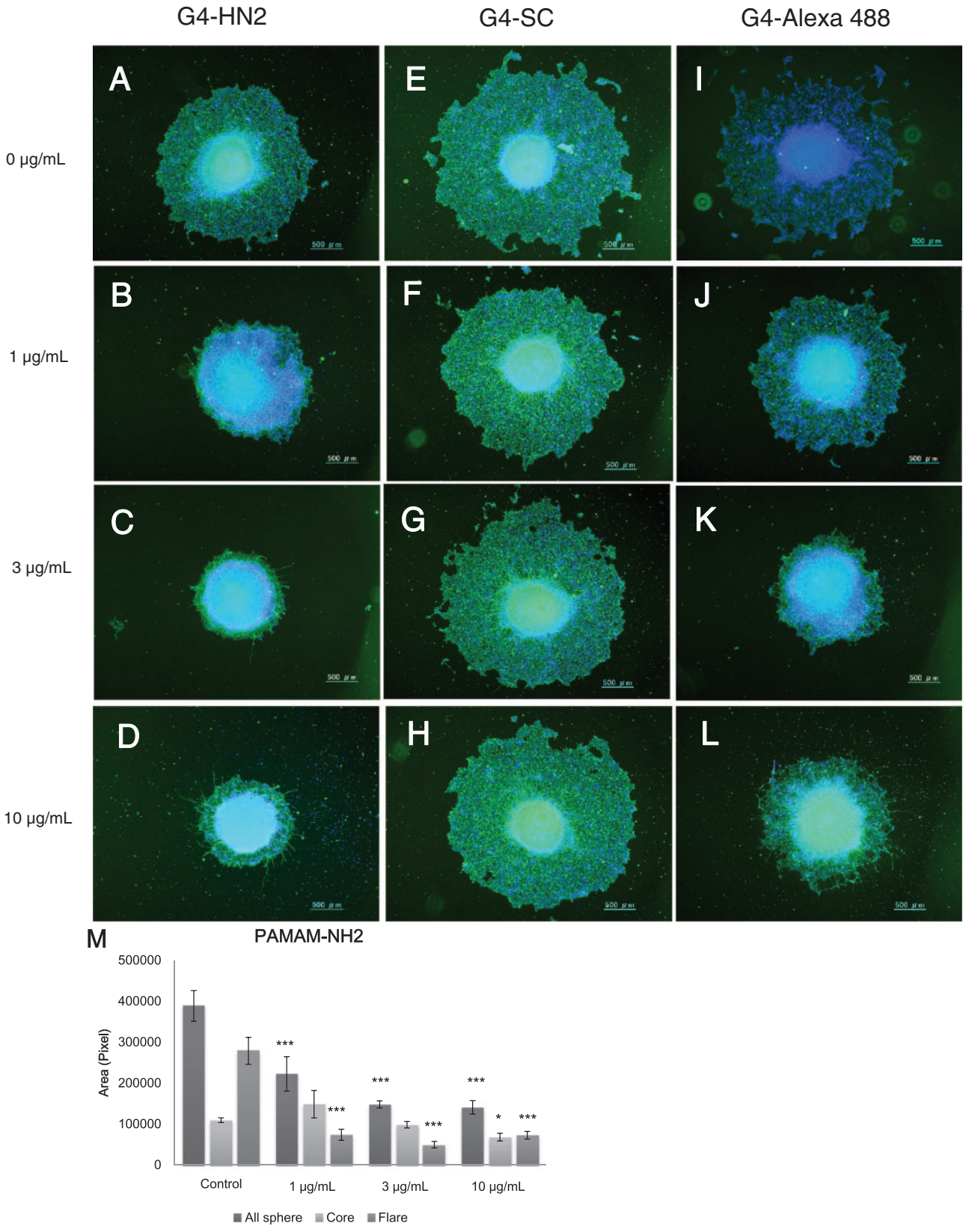

FIG. 6. Effects of PAMAM dendrimers on the migration and differentiation of neurospheres. Representative images were acquired on day 10 for groups of cells treated with PAMAM G4-NH_2 (**B–D**), PAMAM-SC (**F–H**), or Alexa 488-labeled PAMAM-NH_2 (**J–L**) at concentrations of 1, 3, or 10 µg/mL for 72 h and without PAMAM treatment (vehicle control, **A, E** and **I**). Quantified data on the effects on migration of PAMAM-NH_2 were acquired using Image J by measuring both sphere area and flare area (**M**). Data are expressed as the percentage of control ± SD for four independent experiments. $^{*}P < 0.05$ and $^{***}P < 0.001$ were considered to be statistically significant differences between the treatment group and the vehicle control.

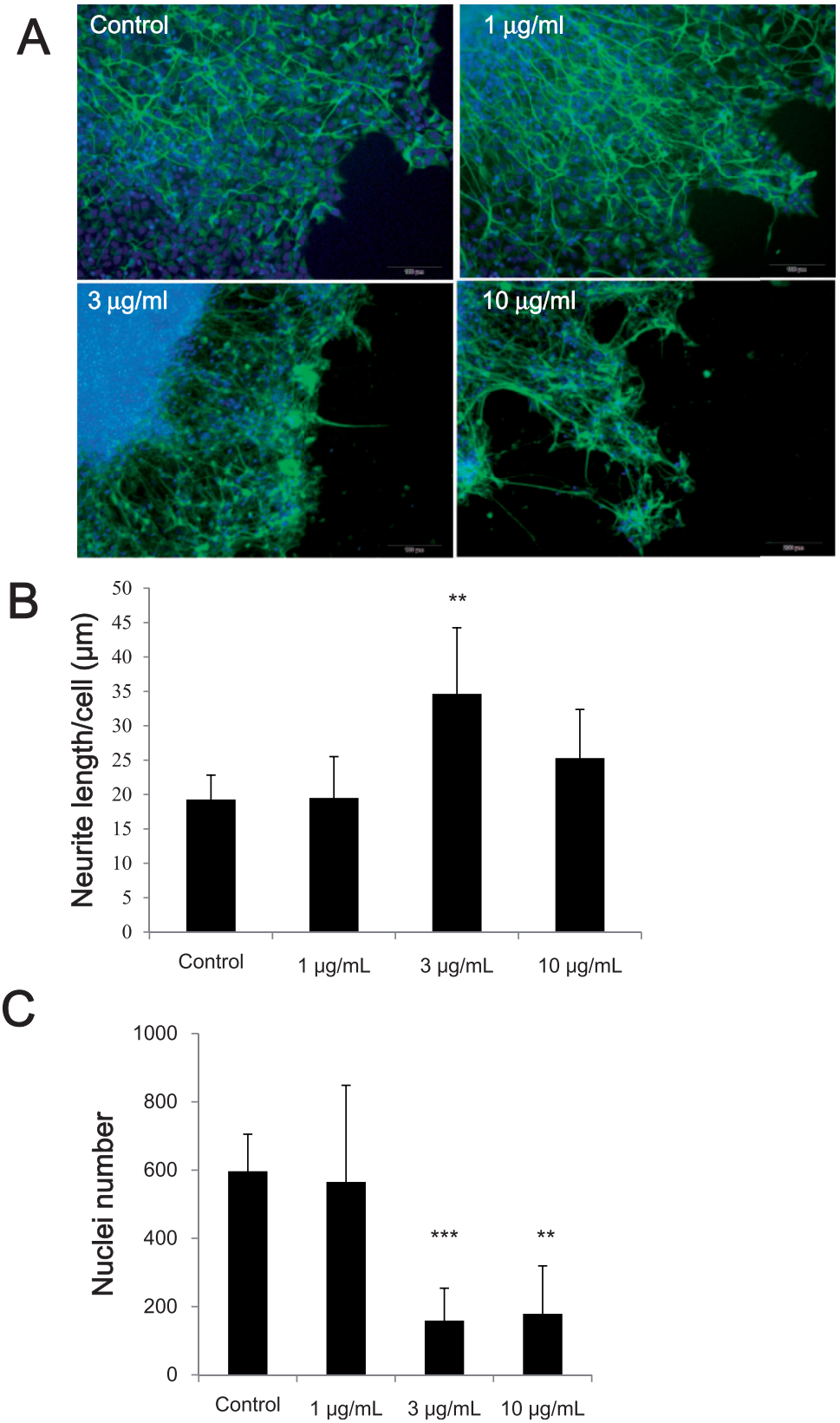

FIG. 7. Images and quantified data of neurite length and nuclei number after PAMAM-NH_2 treatment were measured using the InCell analyzer 1000. The morphology of neuronal cells at 10× magnification was acquired **(A)**. Neurite lengths **(B)** and nuclei number **(C)** were measured. Data are expressed as the percentage of control ± SD for 3 independent experiments. $^{**}P < .01$, and $^{***}P < .001$ were considered to be statistically significant differences between the treatment group and the vehicle control.

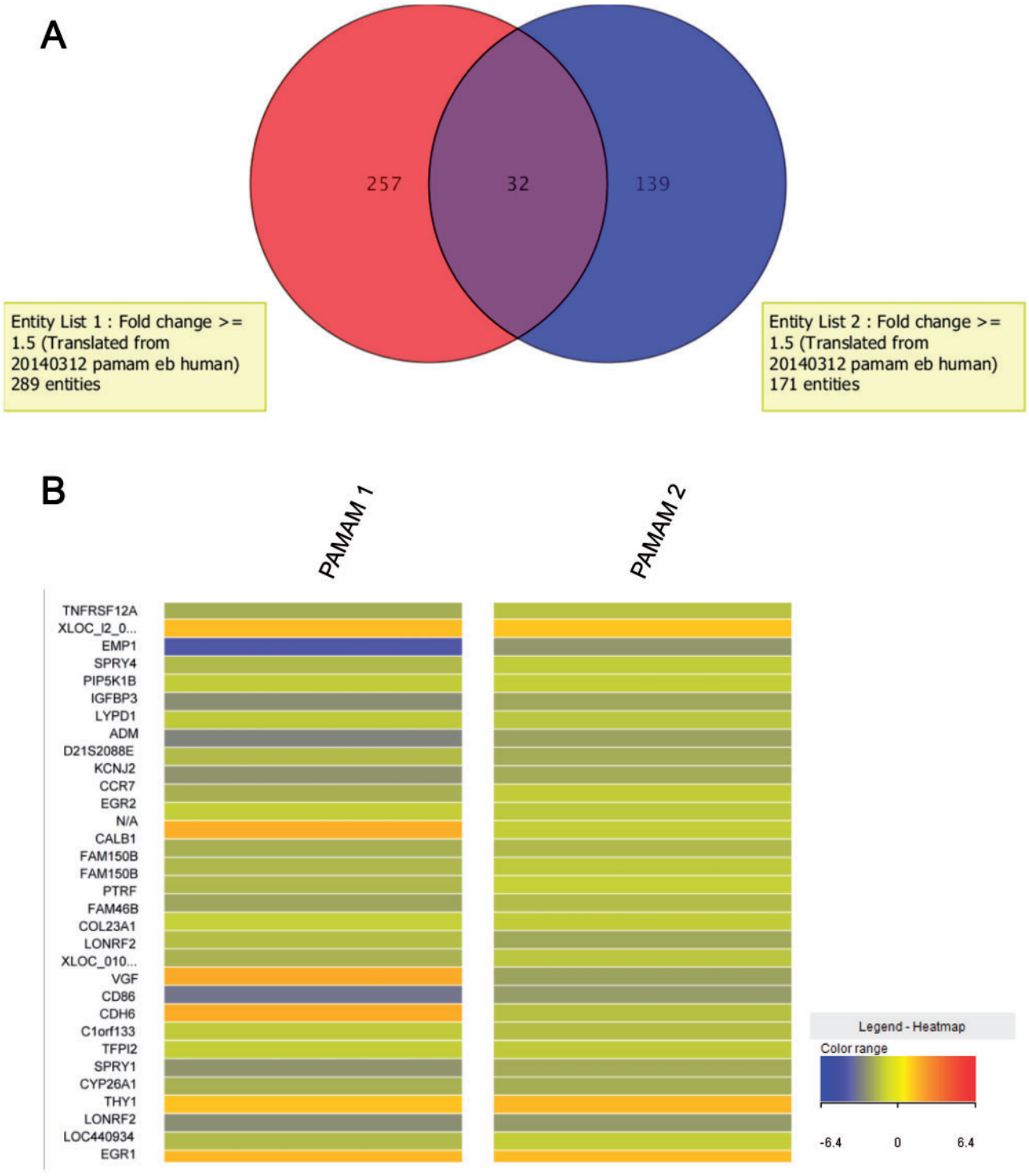

FIG. 8. Gene expression profiling affected by exposure to PAMAM-NH_2 dendrimers. Venn diagram of affected genes **(A)**. Histograms of fold change of 32 commonly regulated genes **(B)**. Each histogram represents the independent cultured sample.

cytotoxicity in a 2D cell culture model (Ciolkowski *et al.*, 2013; Petit *et al.*, 2012). Our previous study suggests that zeta potential of dendrimers is correlated with hNPCs cytotoxicity (Zeng *et al.*, 2016a,b). It has recently been suggested that the exposure of PAMAM dendrimers to animals induces surface chemistry-dependent central neural cytotoxicity, whereas penetration into living neurons was observed after intraparenchymal or intraventricular injection of these molecular complexes (Albertazzi *et al.*, 2013). This is the first study to show that PAMAM dendrimer-NH_2 can influence development in a 3D culture model. The 3D culture model consists of embryoid bodies that closely mimic endogenous developmental processes (Cameron *et al.*, 2006; Weitzer, 2006). Therefore, this model can be used to assess the neurotoxicity of PAMAM dendrimers.

Because PAMAM can be used as a drug carrier to reach an intracellular localization after intracerebroventricular injection,

TABLE 3. Functional Annotation Pathway Listed by Pathway Analysis

Functional Annotated Pathways	P-Value	Matched Gene Entities	Gene entities in the Pathway
Direct interactions	4.09E-10	8	371
Network targets and regulators	1.66E-08	8	407
Hs_Adipogenesis_WP236_44941	0.004330664	2	131
Hs_Myometrial_Relaxation_and_Contraction_Pathways_WP289_45373	0.006092515	2	156
Hs_Regulation_of_Insulin-like_Growth_Factor_(IGF)_Activity_by_Insulin-like_Growth_Factor_Binding_Proteins_(IGFBPs)_WP1899_45051	0.007499467	1	10

Table 4. Pathway Analyses after Exposure to PAMAM Dendrimer

Direct Interactions		
Genes	Log2 FC in group 1	Log2 FC in group 2
KCNJ2	−2.60878	−2.05248
CDH6	−0.86514	−1.05402
EGR1	−2.51403	−2.58341
FAM150B	−1.78654	−1.25689
TFPI2	−2.58243	−2.02963
SPRY4	−1.32929	−0.60296
SPRY1	−1.45947	−1.79482
PIP5K1B	−1.41139	−1.50384
Network Targets and Regulators		
Genes	Log2 FC in group 1	Log2 FC in group 2
CDH6	−0.86514	−1.05402
SPRY4	−1.32929	−0.60296
PIP5K1B	−1.41139	−1.50384
TFPI2	−2.58243	−2.02963
FAM150B	−1.78654	−1.25689
KCNJ2	−2.60878	−2.05248
SPRY1	−1.45947	−1.79482
IGFBP3	−2.7288	−2.14658
Hs_Adipogenesis_WP236_44941		
Genes	Log2 FC in group 1	Log2 FC in group 2
CYP26A1	1.3427806	1.5846124
EGR2	−1.2301817	−1.3729668
Hs_Myometrial_Relaxation_and_Contraction_Pathways_WP289_45373		
Genes	Log2 FC in group 1	Log2 FC in group 2
ADM	−2.976252	−2.2459536
IGFBP3	−2.7287993	−2.146575

Gene expression was shown as the log fold change relative to the control level. The highlighted genes are repeatedly appeared in pathways.

we used hNPCs to study the effects of G4-PAMAM dendrimers on neuronal differentiation. hNPCs were exposed to various concentrations of dendrimers for 72 h and then allowed to differentiate for additional 5 days. PAMAM were observed in neurospheres after 2 days of exposure, indicating that PAMAM dendrimer nanoparticles can penetrate into neurospheres. After 5 days of differentiation, surface type-dependent developmental neurotoxicity effects were observed. Cationic NH_2 but not anionic SC surface functional group dendrimers inhibited cell migration and proliferation but not the differentiation of neurospheres. Gene expression was analyzed after PAMAM exposure. *TFPI2*, *IGFBP3*, and *EGR1* were shown as key nodes in network analysis, suggesting that the restrained expression of these genes plays a very important role after exposure to PAMAM dendrimers.

The physio-chemical characteristics of nanoparticles usually play important roles in their effects on biological systems. PAMAM-SC, PAMAM-NH_2, and PAMAM-Alexa showed a similar size distribution pattern (Table 1). However, PAMAM-NH_2 but not PAMAM-SC inhibited cell proliferation and migration (Figure 6). It was suggested that the surface functional group of the PAMAM dendrimer is more important than particle size in understanding cytotoxicity.

It is important to understand the drug delivery system of dendrimers in the human body. The biodistribution of PAMAM dendrimers has been studied in both mice and rabbits (Lesniak *et al.*, 2013; Opina *et al.*, 2014; Zhao *et al.*, 2014). In this study, we simulated human tissue development using a 3-D culture system to study the biodistribution of dendrimers. We used dendrimer-Alexa conjugates to track PAMAM dendrimers after exposure to neurospheres. PAMAM dendrimers were only observed on the surface of neurospheres during the initial 24 h of exposure; however, conjugates were observed in neurospheres 2 days after exposure. Our finding indicates that PAMAM

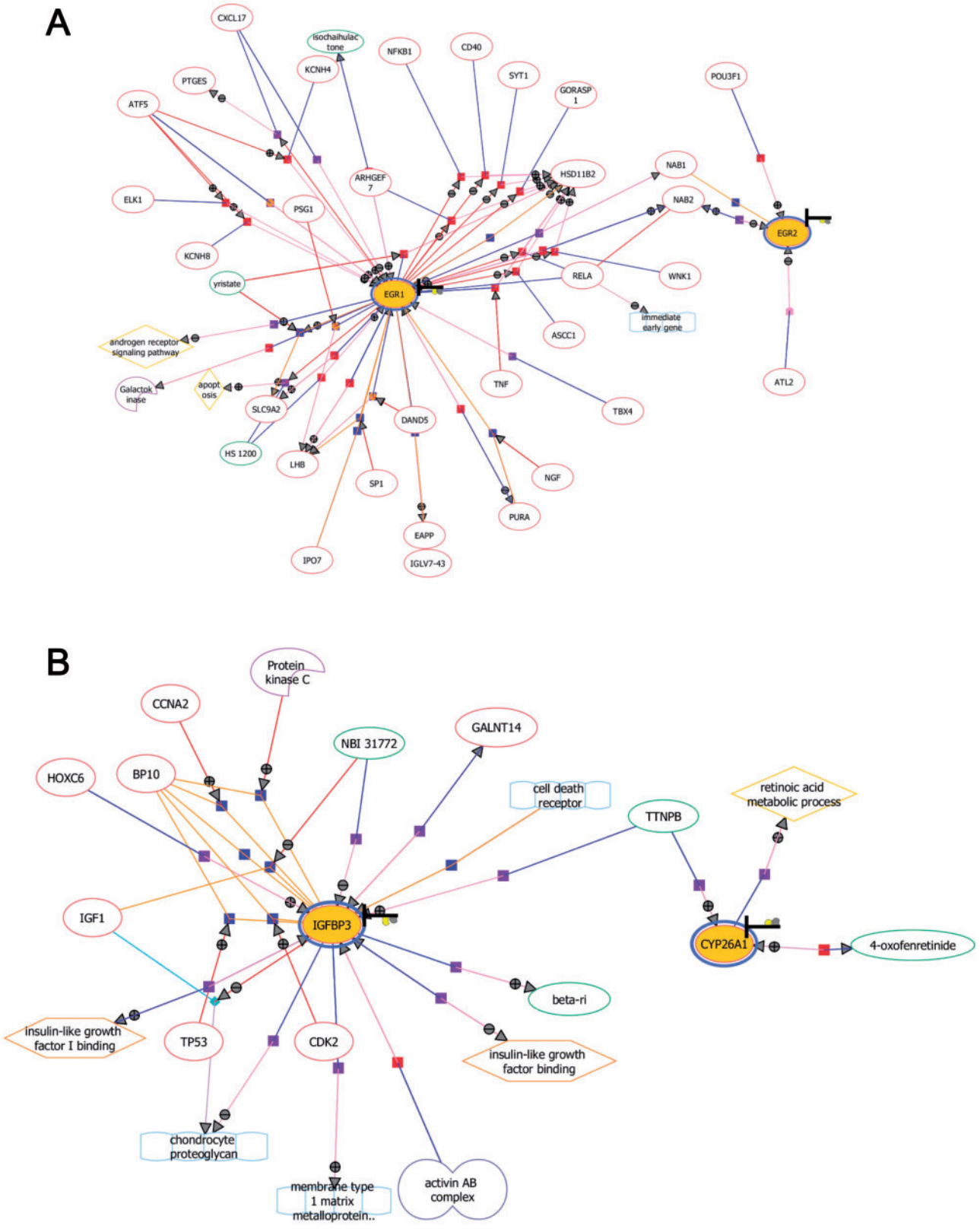

FIG. 9. Network analysis of genes with >1.5-fold changes selected from the microarray analysis. Matched gene entities from the top 5 pathways as shown in Table 2 were then analyzed using NLP) network analyses from GeneSpring to find expanded interactions for EGR1 **(A)**, IGFBP3 **(B)**, TFPI2, and ADM **(C)**.

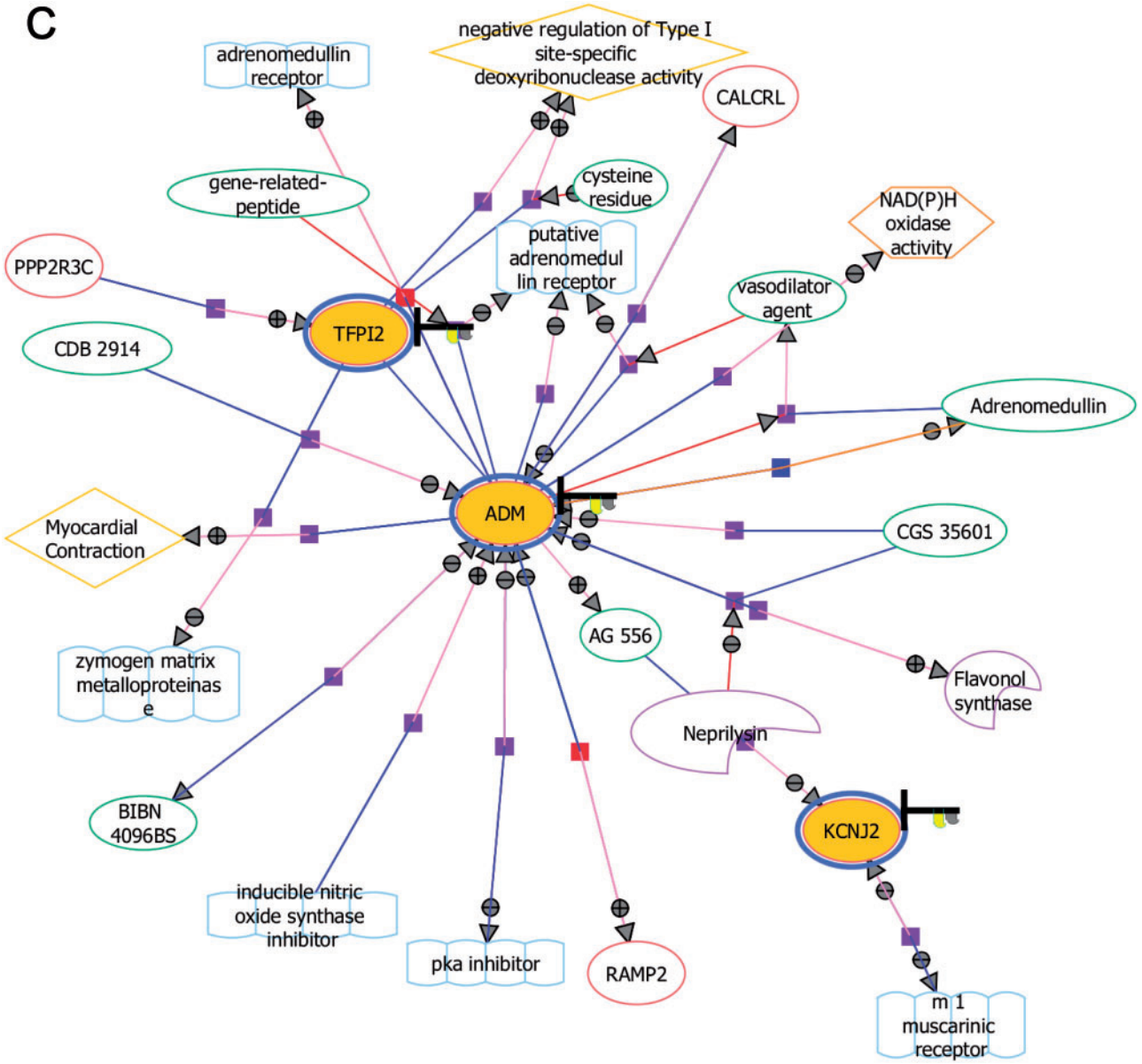

FIG. 9. *Continued*

dendrimer nanoparticles can penetrate into neurospheres through a superficial layer of cells.

Neurospheres were allowed to differentiate for additional 5 days in NDM, and neurite extension and differentiation were studied because they play a very important role during neurodevelopment. PAMAM-SC did not affect neurospheres at any test concentration (Figs. 6E–H). PAMAM-NH_2 significantly inhibited neurosphere flare areas, indicating areas of cell migration and proliferation, at concentrations of 1, 3, and 10 μg/ml (Figure 6M). PAMAM-NH_2 did not inhibit neurite length per cell at any concentration tested in this study. In contrast, neurite length per cell significantly increased at a concentration of 10 μg/ml (Figure 7B), and this may have been because of the PAMAM-induced decrease in the number of live cells (Figure 7C). The cell proliferation assay was performed using NEM after PAMAM exposure. Neurosphere proliferation and migration was inhibited for PAMAM-NH_2 at a concentration of 1, 3, and 10 μg/ml (Figure 4). To confirm the inhibitory effect on cell proliferation, high magnification images (10×) were acquired (Figure 5). The proliferation of cells in the flare areas, which shifted from the neurosphere core, was investigated. EdU-positive cells significantly decreased in the flare area, suggesting that PAMAM dendrimers inhibit both cell migration and proliferation. These results suggested that PAMAM may inhibit cell viability through cell proliferation and migration. However, after PAMAM exposure on neurosphere, no persistent effect on neurite extension of neurosphere was observed, suggesting that PAMAM dendrimers do not have a specific development neurotoxicity effect.

Microarray analysis following PAMAM exposure showed a down regulation of *EGR1*, which plays an important role in regulating cell proliferation and differentiation (Guo *et al.*, 2014), although overexpression of *EGR1* has been shown to induce the osteogenic differentiation of dental stem cells by regulating the expression of *DLX3* and *BMP2* (Press *et al.*, 2015). Egr1 is one of the key transcription factors in extremely low frequency electromagnetic field (ELF-EMF)-induced neuronal differentiation (Seong *et al.*, 2014). The

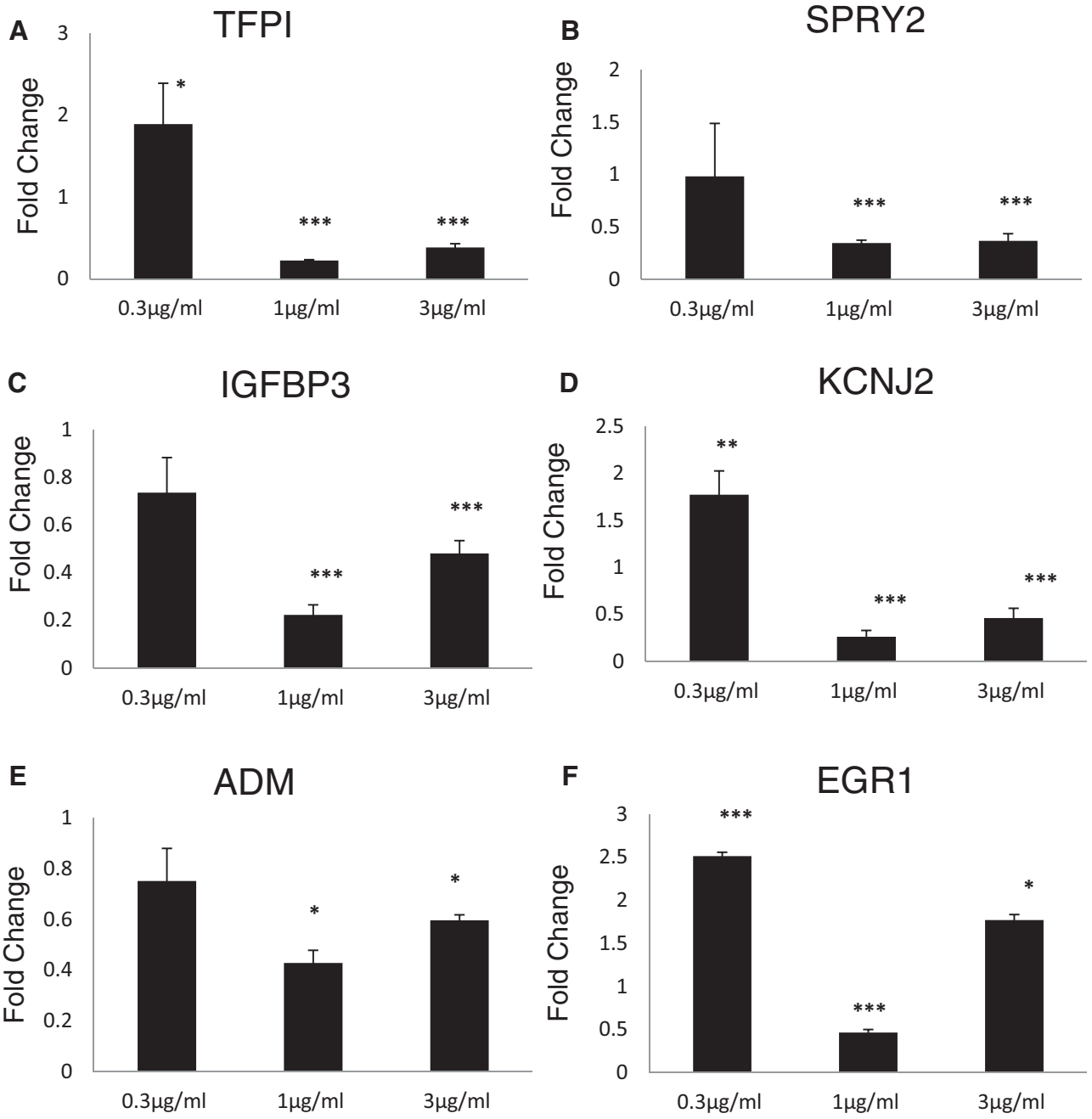

FIG. 10. The expression of selected genes was analyzed by RT-PCR. Results of PAMAM treatment groups were relative to controls set as one. *$P < .05$, **$P < .01$, and ***$P < .001$ were considered to be statistically significant differences between the treatment group and the vehicle control.

observed down regulation of *EGR1* in this study may be because of the positive charge of the PAMAM dendrimer-NH2, which may influence ELF-EMF and induce neuronal migrations. *Spry1* may contribute to congenital disorders involving tissues of neural crest origin (Yang *et al.*, 2010). Down regulation of Spry1 revealed that PAMAM dendrimer exposure during neural development may lead to congenital disorders. Overexpression of *CYP26A1* induces neurodegenerative diseases by the enhancement of retinoic acid (RA) metabolites (Ricard and Gudas, 2013). Cationic PAMAM induces the overexpression of *CYP26A1*, which is considered as a potential risk for inducing some neural toxicity in the human brain. The observed down regulation of genes mostly related to direct interactions and network targets and regulators pathways has revealed that PAMAM dendrimers affect regulator function through a direct interaction. Genes with similar functions usually fall into the same functional modules. We analyzed whether the revealed genes connected with each other using a bioinformatics approach. *EGR1*, *TFPI2*, *IGFBP3*, and *ADM* were found to be the key nodes in their respective networks in the NLP analysis. Because the NLP analysis is based on information from published articles, there is currently no information about these 3 particular networks yet. Therefore, the expression of these genes was then analyzed by RT-PCR, which showed that most of the genes were down regulated in this study. It is suggested that the positive charge of PAMAM

dendrimer-NH2 influences ELF-EMF and inhibits neuronal proliferation.

In conclusion, PAMAM-SC did not affect neurospheres at any test concentration. PAMAM-NH_2 can penetrate into neurospheres in a time-dependent manner. After neurosphere was exposed to 10 μg/ml of PAMAM dendrimers-NH_2 for 72 h, microarray gene pathway analyses revealed a change in the regulation of various genes, including those involved in various signal transduction pathways, and direct interactions and network pathways were the most related. Network analysis using a bioinformatics approach revealed that *TFPI2*, *IGFBP3*, and *EGR1* play a crucial role after exposure to PAMAM dendrimers. Cell proliferation and migration were significantly inhibited at concentrations of 3 and 10 μg/ml. However, after neurospheres were exposed to PAMAM, no persistent effect on neurite extension was observed. These findings suggest that the exposure of neurosphere to PAMAM dendrimers results in a change in cell proliferation and migration through pathways regulated by *TFPI2*, *IGFBP3*, and *EGR1*.

SUPPLEMENTARY DATA

Supplementary data **are available online at** http://toxsci.oxfordjournals.org/.

ACKNOWLEDGMENTS

We thank Dr Seishiroh Hirano and Dr Zhongfang Lei for conducting this study, thank Dr Daisuke Nakajima, Dr Yayoi Kobayashi for helping with analytical methods, and thank Ryoko Yanagisawa, and Naoko Ueki for their technical assistance.

FUNDING

This work was supported by the Grant-in-Aid for Scientific Research from the Ministry of Education, Science, Culture and Sports of Japan (24241013) to H.S.

REFERENCES

Albertazzi, L., Gherardini, L., Brondi, M., Sulis Sato, S., Bifone, A., Pizzorusso, T., Ratto, G. M., and Bardi, G. (2013). In vivo distribution and toxicity of PAMAM dendrimers in the central nervous system depend on their surface chemistry. *Mol. Pharm.* **10**, 249–260.

Baumann, J., Barenys, M., Gassmann, K., and Fritsche, E. (2014). Comparative human and rat "neurosphere assay" for developmental neurotoxicity testing. *Curr. Protoc. Toxicol.* **59**, 1–12.

Bharatwaj, B., Mohammad, A. K., Dimovski, R., Cassio, F. L., Bazito, R. C., Conti, D., Fu, Q., Reineke, J. J., and da Rocha, S. R. (2014). Dendrimer nanocarriers for transport modulation across models of the pulmonary epithelium. *Mol. Pharm.* **12**, 826–838.

Cameron, C. M., Hu, W. S., and Kaufman, D. S. (2006). Improved development of human embryonic stem cell-derived embryoid bodies by stirred vessel cultivation. *Biotechnol Bioeng* **94**, 938–948. DOI 10.1002/bit.20919.

Ciolkowski, M., Rozanek, M., Bryszewska, M., and Klajnert, B. (2013). The influence of PAMAM dendrimers surface groups on their interaction with porcine pepsin. *Biochim. Biophys. Acta* **1834**, 1982–1987.

Cui, D. M., Xu, Q. W., Gu, S. X., Shi, J. L., and Che, X. M. (2009). PAMAM-drug complex for delivering anticancer drug across blood-brain barrier in-vitro and in-vivo. *Afr. J. Pharm. Pharmacol.* **3**, 227–233.

Dobrovolskaia, M. A., Patri, A. K., Simak, J., Hall, J. B., Semberova, J., De Paoli Lacerda, S. H., and McNeil, S. E. (2012). Nanoparticle size and surface charge determine effects of PAMAM dendrimers on human platelets in vitro. *Mol. Pharm.* **9**, 382–393.

Guo, B., Tian, X. C., Li, D. D., Yang, Z. Q., Cao, H., Zhang, Q. L., Liu, J. X., and Yue, Z. P. (2014). Expression, regulation and function of Egr1 during implantation and decidualization in mice. *Cell Cycle* **13**, 2626–2640.

Hill, E. J., Woehrling, E. K., Prince, M., and Coleman, M. D. (2008). Differentiating human NT2/D1 neurospheres as a versatile in vitro 3D model system for developmental neurotoxicity testing. *Toxicology* **249**, 243–250.

Huang, R. Q., Qu, Y. H., Ke, W. L., Zhu, J. H., Pei, Y. Y., and Jiang, C. (2007). Efficient gene delivery targeted to the brain using a transferrin-conjugated polyethyleneglycol-modified polyamidoamine dendrimer. *Faseb J.* **21**, 1117–1125.

Katare, Y. K., Daya, R. P., Sookram Gray, C., Luckham, R. E., Bhandari, J., Chauhan, A. S., *et al.* (2015). Brain targeting of a water insoluble antipsychotic drug haloperidol via the intranasal route using pamam dendrimer. *Mol. Pharm.* **12**, 3380–3388.

Ke, W. L., Shao, K., Huang, R. Q., Han, L., Liu, Y., Li, J. F., Kuang, Y. Y., Ye, L. Y., Lou, J. N., and Jiang, C. (2009). Gene delivery targeted to the brain using an Angiopep-conjugated polyethyleneglycol-modified polyamidoamine dendrimer. *Biomaterials* **30**, 6976–6985.

Khodadust, R., Unsoy, G., and Gunduz, U. (2014). Development of poly (I:C) modified doxorubicin loaded magnetic dendrimer nanoparticles for targeted combination therapy. *Biomed. Pharmacother.* **68**, 979–987.

Lesniak, W. G., Mishra, M. K., Jyoti, A., Balakrishnan, B., Zhang, F., Nance, E., Romero, R., Kannan, S., and Kannan, R. M. (2013). Biodistribution of fluorescently labeled PAMAM dendrimers in neonatal rabbits: effect of neuroinflammation. *Mol. Pharm.* **10**, 4560–4571.

Mukherjee, S. P., Davoren, M., and Byrne, H. J. (2010a). In vitro mammalian cytotoxicological study of pamam dendrimers - towards quantitative structure activity relationships. *Toxicol In. Vitro* **24**, 169–177.

Mukherjee, S. P., Lyng, F. M., Garcia, A., Davoren, M., and Byrne, H. J. (2010b). Mechanistic studies of in vitro cytotoxicity of poly(amidoamine) dendrimers in mammalian cells. *Toxicol. Appl. Pharmacol.* **248**, 259–268.

Newkome, G. R., Childs, B. J., Rourk, M. J., Baker, G. R., and Moorefield, C. N. (1998). Dendrimer construction and macromolecular property modification via combinatorial methods. *Biotechnol. Bioeng.* **61**, 243–253.

Opina, A. C., Wong, K. J., Griffiths, G. L., Turkbey, B. I., Bernardo, M., Nakajima, T., Kobayashi, H., Choyke, P. L., and Vasalatiy, O. (2014). Preparation and long-term biodistribution studies of a PAMAM dendrimer G5-Gd-BnDOTA conjugate for lymphatic imaging. *Nanomedicine* **10**, 1423–1437.

Petit, A. N., Debenest, T., Eullaffroy, P., and Gagne, F. (2012). Effects of a cationic PAMAM dendrimer on photosynthesis and ROS production of Chlamydomonas reinhardtii. *Nanotoxicology* **6**, 315–326.

Press, T., Viale-Bouroncle, S., Felthaus, O., Gosau, M., and Morsczeck, C. (2015). EGR1 supports the osteogenic differentiation of dental stem cells. *Int. Endod. J.* **48**, 185–192.

Ricard, M. J., and Gudas, L. J. (2013). Cytochrome p450 cyp26a1 alters spinal motor neuron subtype identity in differentiating embryonic stem cells. *J. Biol. Chem.* **288**, 28801–28813.

Schulpen, S. H., Pennings, J. L., and Piersma, A. H. (2015a). Gene expression regulation and pathway analysis after valproic acid and carbamazepine exposure in a human embryonic stem cell based neuro-developmental toxicity assay. *Toxicol. Sci.* **146**, 311–320.

Schulpen, S. H., de Jong, E., de la Fonteyne, L. J., de Klerk, A., and Piersma, A. H. (2015b). Distinct gene expression responses of two anticonvulsant drugs in a novel human embryonic stem cell based neural differentiation assay protocol. *Toxicol. In Vitro* **29**, 449–457.

Seong, Y., Moon, J., and Kim, J. (2014). Egr1 mediated the neuronal differentiation induced by extremely low-frequency electromagnetic fields. *Life Sci.* **102**, 16–27.

Win-Shwe, T. T., Sone, H., Kurokawa, Y., Zeng, Y., Zeng, Q., Nitta, H., and Hirano, S. (2014). Effects of PAMAM dendrimers in the mouse brain after a single intranasal instillation. *Toxicol Lett.* **228**, 207–215.

Weitzer, G. (2006). Embryonic stem cell-derived embryoid bodies: an in vitro model of eutherian pregastrulation development and early gastrulation. *Handb. Exp. Pharmacol.* 21–51.

Yang, X., Kilgallen, S., Andreeva, V., Spicer, D. B., Pinz, I., and Friesel, R. (2010). Conditional expression of Spry1 in neural crest causes craniofacial and cardiac defects. *BMC Dev. Biol.* **10**, 48.

Zhao, H., Gu, W., Ye, L., and Yang, H. (2014). Biodistribution of PAMAM dendrimer conjugated magnetic nanoparticles in mice. *J. Mater. Sci. Mater. Med.* **25**, 769–776.

Zeng, Y., Wang, Y., Zeng, Q., Nansai, H., Zhang, Z. Y., and Sone, H. (2015). Optimization of neurosphere assays using human neuronal progenitor cells for developmental neurotoxicity testing. *Am. J. Tissue Eng Stem Cell* **2**, 7–18.

Zeng, Y., Kurokawa, Y., Win-Shwe, T., Zeng, Q., Hirano, S., Zhang, Z. Y., and Sone, H. (2016). Effects of PAMAM dendrimers with various surface functional groups and multiple generations on cytotoxicity and neuronal differentiation using human neural progenitor cells. *J. Toxicol. Sci.*, in press.